Metabolite Profiling of *Panax notoginseng* Using UPLC–ESI-MS

By: Mo Dan, Mingming Su, Xianfu Gao, Tie Zhao, Aihua Zhao, Guoxiang Xie, Yunping Qiu, Mingmei Zhou, Zhong Liu, and Wei Jia

Dan, M., Su, M., Gao, X., Zhao, T., Zhao, A., Xie, G., Qiu, Y., Zhou, M., Liu, Z., & Jia, W. (2008). Metabolite profiling of *Panax notoginseng* using UPLC-ESI-MS. *Phytochemistry*, *69*, 2237-2244.

Abstract:
The metabolite profiling of different parts of *Panax notoginseng* was carried out using rapid ultra-performance liquid chromatography–electrospray ionization mass spectrometry (UPLC–ESI-MS) and multivariate statistical analysis. Principal component analysis (PCA) of the UPLC–ESI-MS data showed a clear separation of compositions among the flower buds, roots and rhizomes of *P. notoginseng*. The saponins accounting for such variations were identified through the corresponding loadings weights and were further verified by accurate mass, tandem mass and retention times of available standard saponins using UPLC quadrupole time-of-flight mass spectrometer (UPLC–QtofMS). Finally, the influential factors of different metabolic phenotypes of *P. notoginseng* was elucidated. The currently proposed UPLC–ESI-MS/MS analytical method coupled with multivariate statistical analysis can be further utilized to evaluate chemical components obtained from different parts of the plant and/or the plant of different geographical locations, thereby classifying the medicinal plant resources and potentially elucidating the mechanism of inherent phytochemical diversity.

Article:
INTRODUCTION
According to the World Health Organization (WHO), about 65–80% of the world's population is using herbal medicine as the primary form of healthcare (Akerele, 1992). *Panax notoginseng* (Burk.) F.H. Chen (Araliaceae) (Sanqi or Tianqi in Chinese) is a highly valuable and important tonic herb cultivated mainly in Yunnan province, PR China. Extensive phytochemical and pharmacological studies on *P. notoginseng* (Wang et al., 2006a and Wang et al., 2006b) have isolated and characterized a total of 56 dammarane-type saponins, most of which have proved to be bioactive for prevention and treatment of cardiovascular and cerebrovascular diseases (Cicero et al., 2003 and Ma et al., 1998), immunoregulation (Sun et al., 2006), hepatoprotection (Ng, 2006), and anti-carcinogenesis (Konoshima et al., 1999). Specifically, ginsenoside Rb_3, one of 20(S)-protopanaxadiol type saponins (Taniyasu et al., 1982 and Xiao, 2002), with a high concentration in the flower buds, exhibited a strong neuroprotective effect (Xu et al., 2005), whereas ginsenoside Rb_1 present mainly in the root has been reported to protect against free

radical damage, maintain normal cholesterol levels and blood pressure, and inhibit the induction phase of long-term potentiation induced by high-frequency stimulation in the dentate gyrus of anesthetized rats in a dose-dependent manner (Wang and Zhang, 2003). These saponins in the different parts of *P. notoginseng* including roots, rhizomes and flower buds, 'either alone or in combination', account for diverse therapeutic effects. Thus understanding the bio-distribution of these secondary metabolites in different parts of *P. notoginseng* is paramount for the investigation of their pharmacological efficiency (Wang et al., 2005).

Metabolites are the end products of cellular regulatory processes, and their fluxes and levels can be regarded as the ultimate response of biological systems to control genetic or environmental changes (Fiehn, 2002). Selectively monitoring important metabolites derived from a biological system allows phytochemists to depict the inherent similarities and differences among the various plants and the various parts of the same plant (Wang et al., 2004b). In parallel with the flourish of 'transcriptome' and 'proteome' in the functional genomic era, metabolomics or metabolite profiling, aiming to identifying and quantifying the entire spectrum of the metabolites in biological systems, has aroused extensive awareness and interests (Rochfort, 2005), especially in the botanical studies such as quality control of plants (Chang et al., 2006, Huhman and Sumner, 2002 and IIka et al., 2007), plant engineering (Anterola and Lewis, 2002 and Long et al., 2006), and clinical trials (Dong and He, 2006). To date, high performance liquid chromatography–mass spectrometry (HPLC–MS) (Murch et al., 2004) and gas chromatography–mass spectrometry (GC–MS) (Farag et al., 2007 and Fukusaki et al., 2006) have been widely employed for high-throughput metabolite profiling strategy. Recently, the soaring development of column particle materials has highlighted a new addition to chromatographic separation technology, the ultra-performance liquid chromatography (UPLC), which allows satisfactory separation, good resolution and sensitivity, and high-speed detection (Wilson et al., 2005) with complex biological samples, such as herbal medicine (Guan et al., 2007). The UPLC coupled with MS has become a more powerful tool to simultaneously identify and quantify the complicated components in herbal medicine (Chan et al., 2007).

In this paper, we describe a high-throughput and reliable UPLC–ESI-MS-based analytical method in association with principal component analysis (PCA) to profile and discriminate the samples from different parts of *P. notoginseng*. Accurate mass and tandem mass were used to identify these significantly altered compositions with bioactivity present in different parts of *P. notoginseng* using UPLC–QtofMS. Further, we identified the tentative mechanism of metabolic outcomes diversity.

RESULTS AND DISCUSSION

Saponins profiling of different parts of P. notoginseng

As compared with simultaneous determination of several saponins in *P. notoginseng*, (Li et al., 2005a, Liu et al., 2004, Wang et al., 2006a and Wang et al., 2006b), the metabolite profiling study requires higher resolution and sensitivity. UPLC–ESI-MS system was employed to provide a rapid, effective, and convenient profiling analytical method for a wide range of saponins present in *P. notoginseng*. Theoretically, a higher flow rate (above 0.6 ml/min) promises a good separation using UPLC, whereas the flow rate for the electrospray source is below 1.0 ml/min. Meanwhile, flow into the ion source should be limited within 0.2 ml/min, so as to guarantee the ionization efficiency and ameliorate ion suppression which significantly reduces analytical

sensitivity. Considering sensitivity and resolution together, the ultimate flow rate was optimized at 0.35 ml/min throughout the study. In addition, the effects of formic acid at different concentrations (0.1%, 0.05% and 0.01%) were tested, and 0.01% formic acid exhibited good separation with slight reduction of peak signal. The column temperature was set at 40 °C to alleviate extra column pressure resulting from a higher flow rate, which can improve chromatographic separation and peak shape. Isocratic elution commonly led to the overlapped peaks mainly due to similar polarity and structure of most ginsenosides; hence gradient elution was adopted to obtain better separation and lower LOQ. Compared with pervious HPLC research suffering long run time as long as 50 min (Li et al., 2005b), the major saponins were excellently separated as well as superior peak shape, especially fourteen saponins quantified during 21 min.

More information on saponins was obtained in the ES+ mode than ES− mode due to higher degree of ion fragmentation as revealed by the representative total ion current (TIC) spectra on the UPLC–ESI-MS. Despite of the coexistence of three major fragment ions $[M+Na]^+$, $[M+K]^+$, and $[M+H]^+$, we adopted the adduct ion of $[M+Na]^+$ as the target *m*/*z* in terms of the abundance and constant of $[M+Na]^+$, which was reported in *P. ginseng* (Cui et al., 2001 and Liu et al., 2006). The desolvation gas flow was set at 600 l/h, cone gas flow at 50 l/h, and desolvation temperature at 300 °C, respectively, so as to remove redundant solvent resulting from a higher flow rate of 0.35 ml/min for single quadrupole mass spectrometer. Cone voltage was optimized to the corresponding values ranging from 25 V to 90 V owing to the broad range of molecular weight of saponins (400–1400 Da). The simultaneous separation and detection of the metabolites using UPLC–ESI-MS required an analytical method with high precision, repeatability, and recovery. In general, the proposed method exhibits reliable accuracy, and good reproducibility (Stable 1).

Visual inspection of UPLC–ESI-MS spectra

Most of the 14 reference standards (Fig. 1) were readily identified within the UPLC–ESI-MS spectra of roots, rhizomes and flower buds of *P. notoginseng* via paired retention time and mass to charge ratio (paired Rt−*m*/*z*). Visual inspection of the spectra from the different parts of *P. notoginseng* revealed a salient difference with each other. The ginsenoside Rb_3 concentration was relatively higher in the flower bud than in the root while the content of ginsenoside Rg_1 was higher in the root and rhizome than in the flower bud and ginsenoside F_1 can barely be detected in the flower bud, etc. These findings indicated that there existed different kinds of saponins with diverse concentrations in the different parts of *P. notoginseng*. However, for further interpretation of the variations among samples from different parts of the plant, multivariate statistical analysis such as PCA was employed in this study.

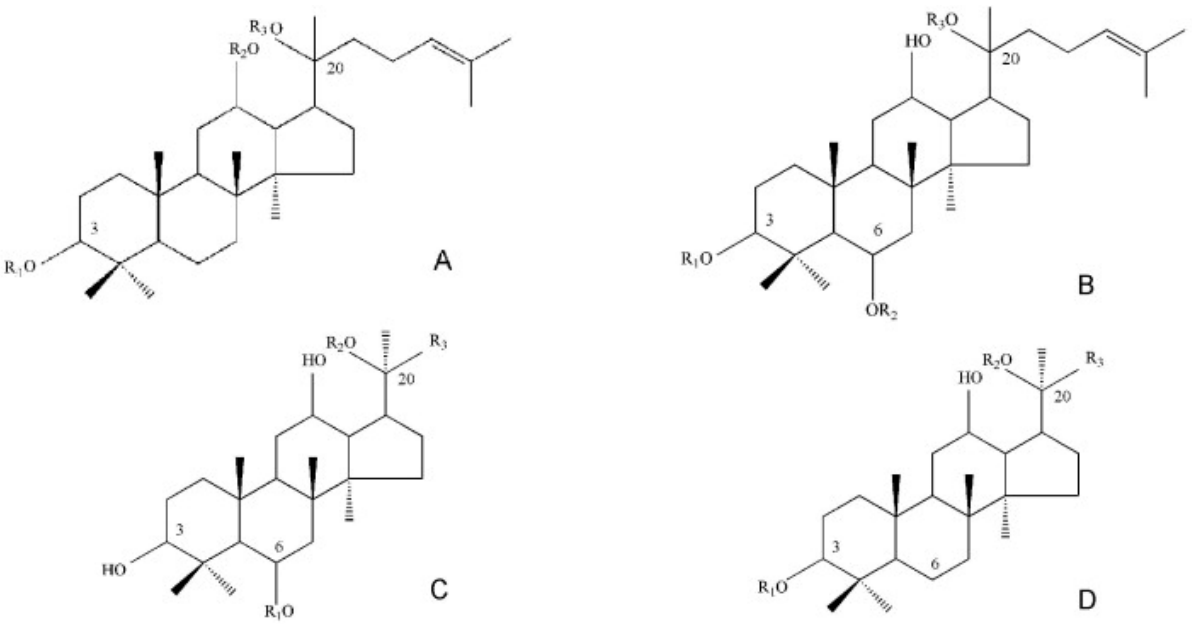

Type		Saponins	R_1	R_2	R_3	Molecular formula
Type A	1	Malonyl-ginsenoside-Rb_1	-Glc^2-Glc^6-Malonyl	-H	-Glc^6-Glc	$C_{57}H_{94}O_{26}$
	2	Notoginsenoside-R_4	-Glc^2-Glc	-H	-Glc^6-Glc^6-Xyl	$C_{59}H_{100}O_{27}$
	3	Notoginsenoside-Fa	-Glc^2-Glc^2-Xyl	-H	-Glc^6-Glc	$C_{59}H_{100}O_{27}$
	4	Ginsenoside-Rb_1	-Glc^2-Glc	-H	-Glc^6-Glc	$C_{54}H_{92}O_{23}$
	5	Notoginsenoside-Q	-Glc^2-Glc^2-Xyl	-H	-Glc^2-Xyl^4-Xyl	$C_{63}H_{106}O_{30}$
	6	Notoginsenoside-S	-Glc^2-Glc^2-Xyl	-H	-Glc^2-Ara(p)^5-Xyl	$C_{63}H_{106}O_{30}$
	7	Ginsenoside-Rb_2	-Glc^2-Glc	-H	-Glc^6-Ara(p)	$C_{53}H_{90}O_{22}$
	8	Notoginsenoside-Fc	-Glc^2-Glc^2-Xyl	-H	-Glc^6-Xyl	$C_{58}H_{98}O_{26}$
	9	Ginsenoside-Rb_3	-Glc^2-Glc	-H	-Glc^6-Xyl	$C_{53}H_{90}O_{22}$
	10	Ginsenoside-Rc	-Glc^2-Glc	-H	-Glc^6-Ara(f)	$C_{53}H_{90}O_{22}$
	11	Ginsenoside-Rd	-Glc^2-Glc	-H	-Glc	$C_{48}H_{82}O_{18}$
	12	Ginsenoside-F_2	-Glc	-H	-Glc	$C_{42}H_{72}O_{13}$
	13	20(R)-Ginsenoside-Rg_3	-Glc^2-Glc	-H	-H	$C_{42}H_{72}O_{13}$
	14	Ginsenoside-Rh_2	-Glc	-H	-H	$C_{36}H_{62}O_8$
Type B	15	20-O-Glucoginsenoside-Rf	-H	-Glc^2-Glc	-Glc	$C_{48}H_{82}O_{19}$
	16	Notoginsenoside-R_1	-H	-Glc^2-Xyl	-Glc	$C_{47}H_{80}O_{18}$
	17	Ginsenoside-Rg_1	-H	-Glc	-Glc	$C_{42}H_{72}O_{14}$
	18	Ginsenoside-Re	-H	-Glc^2-Rha	-Glc	$C_{48}H_{82}O_{18}$
	19	Notoginsenoside-R_2	-H	-Glc^2-Xyl	-H	$C_{41}H_{70}O_{13}$
	20	Ginsenoside-Rf	-H	-Glc^2-Glc	-H	$C_{42}H_{72}O_{14}$
	21	Ginsenoside-Rg_2	-H	-Glc^2-Rha	-H	$C_{42}H_{72}O_{13}$
	22	Ginsenoside-F_1	-H	-H	-Glc	$C_{36}H_{62}O_9$
Type C	23	Notoginsenoside-H	-Glc^2-Xyl	-Glc	$C_6H_{11}O$	$C_{47}H_{80}O_{19}$
Type D	24	Notoginsenoside-A	-Glc^2-Glc	-Glc^6-Glc	$C_6H_{11}O$	$C_{54}H_{92}O_{24}$
	25	Notoginsenoside-B	-Glc^2-Glc	-Glc^6-Glc	C_6H_9O	$C_{54}H_{90}O_{24}$

Figure 1: Saponins **1**–**25** observed by positive-ion UPLC–ESI-MS in *P. notoginseng* (Glc, β-d-glucose; Rha, α-l-rhamnose; Ara(p), α-l-arabinose (pyranose); Ara(f), α-l-arabinose (furanose); Xyl, β-d-xylose).

Principal component analysis

PCA is an unsupervised clustering method requiring little prior knowledge of the data set and acts to reduce the dimensionality of multivariate data without losing important information (Eriksson et al., 2001). Both UV-scaled (scaled to standard deviation) and Par-scaled (scaled to square root of standard deviation) mathematical methods were performed to pre-treat the data sets resulting from roots, rhizomes and flower buds of *P. notoginseng*. The clear separation of the three different parts was observed in the PCA scores plot where each coordinate represents a sample (Fig. 2). Two-component PCA model cumulatively accounted for 80.0% of variation. The flower buds and the others were clearly separated by the principal component 1 (PC1), whereas the roots and rhizomes were readily discriminated by the principal component 2 (PC2). However, the UV-scaled loadings were difficult to be interpreted, because their relative values are strongly distorted by the variance scaling procedure (Cloarec et al., 2005). In this work, therefore, PCA scores plot and loadings plot were achieved using mean-centered, Par-scaled data. The preferential distribution of marker ions in the first quadrant of the loadings plot accounted primarily for the difference of roots. Analogously, the distribution in the second and third quadrants of the loadings plot indicated the variation of rhizomes and flower buds of *P. notoginseng*, respectively.

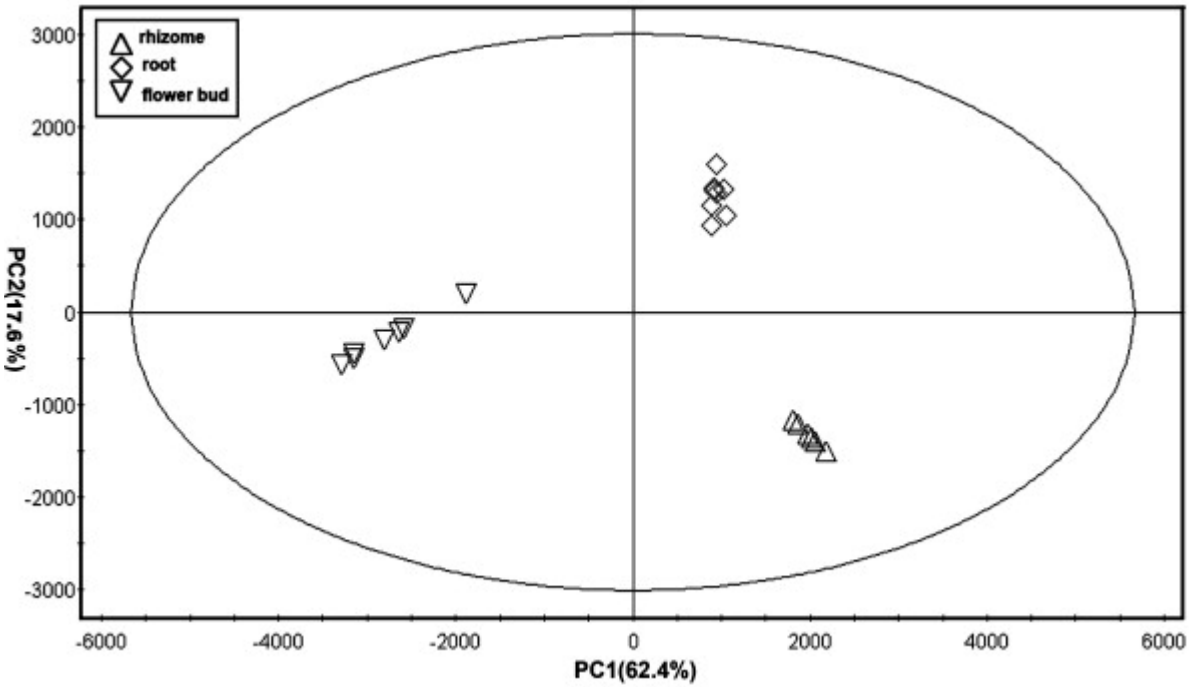

Figure 2: PCA scores plot (PC1 vs. PC2) of 70% methanol extracts of three parts of *P. notoginseng*: seven flower bud samples, eight root samples and six rhizome samples.

Tentative marker assignment

It is possible to determine variable importance by analyzing the correlation between variables in the PC1 and PC2 dimension, a list of marker ions of interest was therefore obtained from the PCA loadings plot (Fig. 3). Marker ions *m/z* 823.8($[M+Na]^+$, Rt 3.59 min), 984.9($[M+Na]^+$, Rt 2.92 min), 1131.8($[M+Na]^+$, Rt 9.31 min), 1145.7($[M+Na]^+$, Rt 7.06 min), and 1147.8($[M+Na]^+$,

Rt 6.76 min) mainly present in the first quadrant are to characterize the roots of *P. notoginseng*. Marker ions 1102.1($[M+Na]^+$, Rt 10.73 min), 1101.9($[M+Na]^+$, Rt 11.85 min), 1365.9($[M+Na]^+$, Rt 9.85 min), 1365.8($[M+Na]^+$, Rt 10.03 min), 1233.8 ($[M+Na]^+$, Rt 11.09 min) and 807.9($[M+Na]^+$, Rt 17.87 min) are far from the centre in the third quadrant of the loadings plot, suggesting that these components exhibit a higher importance in the flower buds than that in the other two parts of *P. notoginseng*. Marker ions 645.8($[M+Na]^+$, Rt 20.17 min), 807.9($[M+Na]^+$, Rt 8.42 min), 823.8($[M+Na]^+$, Rt 7.99 min), 956.4($[M+Na]^+$, Rt 3.35 min), 969.7($[M+Na]^+$, Rt 12.97 min), 979.8($[M+Na]^+$, Rt 3.62 min), 972.1($[M+Na]^+$, Rt 3.40 min), 1102.1($[M+Na]^+$, Rt 12.26 min), 1218.2($[M+Na]^+$, Rt 5.60 min), 1264.3($[M+Na]^+$, Rt 7.55 min) and 1264.5 ($[M+Na]^+$, Rt 8.12 min) are predominant compounds in the rhizomes.

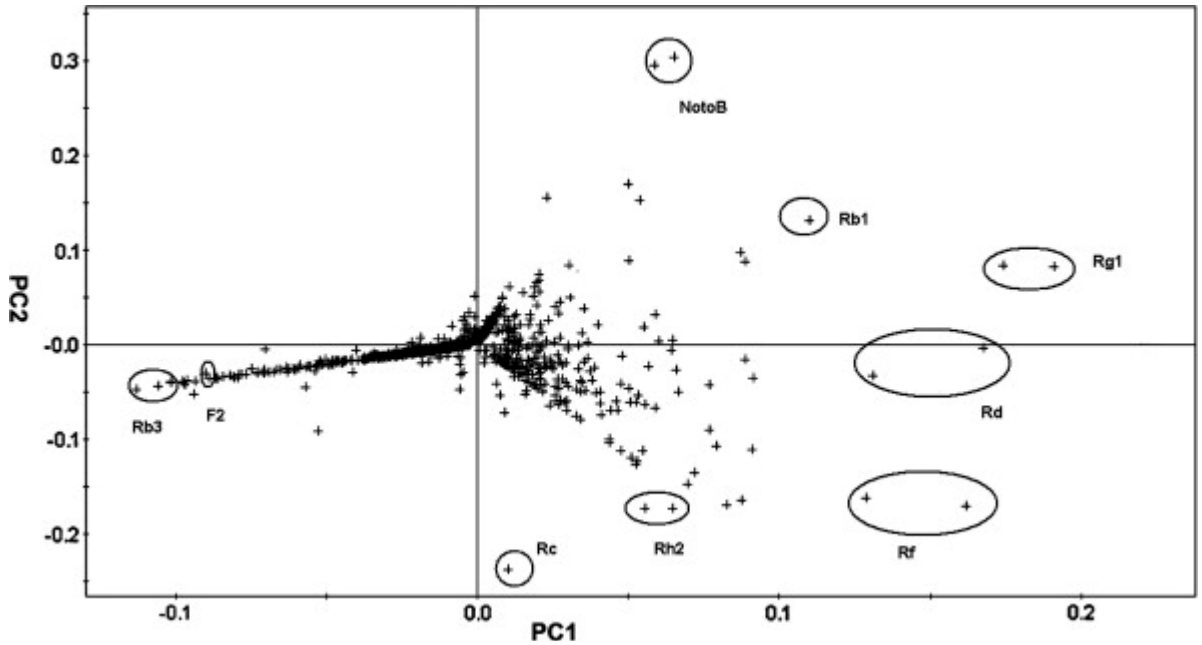

Figure 3: PCA loadings plot of all the UPLC–ESI-MS signals of different parts of *P. notoginseng*.

In order to identify these important marker ions, qualitative analysis of saponins present in the flower buds, roots and rhizomes of *P. notoginseng* was carried out on an UPLC coupled to ESI quadrupole time-of-flight mass spectrometry (UPLC–ESI–QtofMS) in positive mode. Accurate mass measurement was rendered possible by the simultaneous, but independent acquisition of reference ions of leucine-enkephalin via the LockSpray™ interface. This configuration offered several advantages for untargeted metabolite profiling including minimization of ion suppression due to reference ions, prevention of fluctuations in reference ionization efficiency due to gradient elution. Using this approach, improved mass accuracy data were acquired in the range of 0.2–14 ppm, which significantly reduces the number of possible structures of saponins. However, mass accuracy data does not provide sufficient information necessary to distinguish saponins with the same molecular weight, tandem MS and available standards were used to verify these important marker ions. MS/MS analysis of saponins in this study was performed at different collision energies ranging from 6 V to 10 V in order to obtain the more sensitive response for each product ion. A total of 14 saponins (notoginsenoside R_1**16**, R_2**19**, ginsenoside Rb_1**4**, Rb_2**7**,

Rb_3**9**, Rc **10**, Rd **11**, F_2**12**, 20(R)–Rg_3**13**, Rh_2**14**, Rg_1**17**, Re **18**, Rg_2**21**, and F_1**22**) (Table 1) were verified by comparing the accurate mass and retention time with those of standards available, and the contents of these saponins were quantified using corresponding calibration curve of the spiked 14 standards. The remaining 11 marker ions were provisionaly identified as notoginsenoside R_4**2**, Fa **3**, Q **5**, S **6**, Fc **8**, H **23**, A **24**, B **25**, ginsenoside R_f**20**, malonyl-ginsenoside-Rb_1**1** and 20-*O*-glucoginsenoside-R_f**15** using accurate mass and tandem mass spectrometry, further studies should be initiated for identification and quantification of those saponins when the reference standards are available. The improved mass accuracy data and tandem mass data are provided in Table 2. Using such a strategy, ginsenoside Rb_1**4**, Rg_1**17**, notoginsenoside A **24**, B **25** and 20-*O*-glucoginsenoside-R_f**15** are considered as the critical marker ions (compounds) in the roots, which are the main active saponins in the roots of *P. notoginseng*. Notoginsenoside Q **5**, S **6**, Fc **8**, ginsenoside Rb_2**7**, Rb_3**9**, and F_2**12**, tentatively assigned as marker ions, mainly existed in the flower buds of *P. notoginseng*, which were reported by previous studies (Wan et al., 2006 and Yoshikawa et al., 2003). Ginsenoside Re **18**, R_f**20**, Rg_2**21**, notoginsenoside R_1**16**, (protopanaxatriol-type saponins), notoginsenoside R_4**2**, Fa **3**, ginsenoside Rc **10**, Rd **11**, Rh_2**14**, Malonyl-ginsenoside-Rb_1**1** (protopanaxadiol-type saponins) and notoginsenoside H **23** identified in this study are representative ions for rhizome of *P. notoginseng*, which is consistent with the report that the amount of protopanaxatriol-type saponins is higher in the rhizome of *P. notoginseng* than in the root whereas the contents of many protopanaxadiol-type saponins are higher in both the rhizome and flower bud of *P. notoginseng* than in the root (Wei and Du, 1996).

Table 1: The average contents (mg/g) of investigated 14 saponins in different parts of *P. notoginseng*

	Rhizome (*n* = 6)	**Root (*n* = 8)**	**Flower bud (*n* = 7)**
Notoginsenoside R_1(16)	3.64 ± 0.34	2.76 ± 0.26	1.30 ± 0.09
Notoginsenoside R_2(19)	2.79 ± 0.36	1.48 ± 0.70	1.63 ± 0.54
Ginsenoside Rb_1(4)	42.53 ± 9.34	37.67 ± 8.13	53.13 ± 4.67
Ginsenoside Rb_2(7)	0.27 ± 0.02	ND	21.08 ± 2.70
Ginsenoside Rb_3(9)	5.82 ± 0.53	0.79 ± 0.13	55.63 ± 9.39
Ginsenoside Rc (10)	9.96 ± 0.81	0.84 ± 0.32	32.02 ± 11.66
Ginsenoside Rd (11)	7.77 ± 0.55	3.11 ± 0.37	2.54 ± 0.70
Ginsenoside F_2(12)	0.67 ± 0.18	0.40 ± 0.07	3.06 ± 0.21
Ginsenoside 20(R)–Rg_3(13)	1.03 ± 0.07	0.99 ± 0.07	6.90 ± 0.36
Ginsenoside Rh_2(14)	0.14 ± 0.01	ND	ND
Ginsenoside Rg_1(17)	42.10 ± 3.13	44.72 ± 6.30	4.44 ± 0.44
Ginsenoside Re (18)	9.27 ± 0.76	6.22 ± 1.41	1.06 ± 0.05
Ginsenoside Rg_2(21)	1.79 ± 0.42	1.19 ± 0.41	2.28 ± 0.68
Ginsenoside F_1(22)	0.14 ± 0.01	ND	ND

Table 2: Precursor and product ions of the Saponins **1**–**25** in the different parts of *P. notoginseng* using UPLC–QtofMS [*m*/*z* with relative abundance (%) in parentheses]

Compound number	Identification	R_t (min)	Theoretical accurate mass	QtofMS (*m*/*z*)(ESI+)	Mass accuracy (ppm)	MS/MS fragment ion (*m*/*z*)
1	Malonyl-ginsenoside-Rb_1	5.60	1195.6112$[M+H]^+$	1195.6099$[M+H]^+$	1.09	1108.6008(88)$[M+H-Mal]^+$, 946.5451(14)$[M+H-Mal-Glc]^+$, 853.4939(100)$[M+H-GlcGlc-H_2O]^+$, 835.4861(38)$[M+H-GlcGlc-2H_2O]^+$, 785.0267(5)$[M+H-GlcGlc-Mal]^+$
2	Notoginsenoside-R_4	7.55	1241.6530$[M+H]^+$	1241.6539$[M+H]^+$	0.72	1109.63104(75)$[M+H-Xyl]^+$, 1079.6015(100)$[M+H-Glc]^+$, 947.5589(43)$[M+H-Xyl-Glc]^+$, 785.5032(70)$[M+H-Xyl-GlcGlc]^+$
3	Notoginsenoside-Fa	8.12	1241.6530$[M+H]^+$	1241.6538$[M+H]^+$	0.64	1109.6135(100)$[M+H-Xyl]^+$, 1079.6025(37)$[M+H-Glc]^+$, 947.5553(15)$[M+H-Xyl-Glc]^+$, 785.5049(63)$[M+H-GlcXyl-Glc]^+$, 460.6224(23)$[M+H-GlcGlcXyl-GlcGlc]^+$
4	Ginsenoside-Rb_1	9.31	1109.6108$[M+H]^+$	1109.6175$[M+H]^+$	6.04	947.5649(100)$[M+H-Glc]^+$, 785.5129(65)$[M+H-GlcGlc]^+$, 767.5134623(79)$[M+H-GlcGlc-H_2O]^+$, 4621(38)$[M+H-GlcGlcGlc]^+$
5	Notoginsenoside-Q	9.85	1343.6847$[M+H]^+$	1343.6850$[M+H]^+$	0.22	1211.6432(100)$[M+H-Xyl]^+$, 1079.6038(52)$[M+H-XylXyl]^+$, 947.5563(15)$[M+H-XylXyl-Xyl]^+$, 917.5463(56)$[M+H-GlcXyl-Xyl]^+$
6	Notoginsenoside-S	10.03	1343.6847$[M+H]^+$	1343.6841$[M+H]^+$	0.45	1211.6414(35)$[M+H-Xyl]^+$, 1079.6009(100)$[M+H-AraXyl]^+$, 947.5542(26)$[M+H-AraXyl-Xyl]^+$, 785.5043(49)$[M+H-GlcXyl-AraXyl]^+$
7	Ginsenoside-Rb_2	10.73	1079.6002$[M+H]^+$	1079.5970$[M+H]^+$	2.96	947.5519(100)$[M+H-Ara]^+$, 917.5454(44)$[M+H-Glc]^+$, 785.5001(52)$[M+H-Ara-Glc]^+$, 767.4929(21)$[M+H-Ara-Glc-H_2O]^+$, 624.0578(17)$[M+H-Ara-GlcGlc]^+$
8	Notoginsenoside Fc	11.09	1211.6425$[M+H]^+$	1211.6450$[M+H]^+$	2.06	1079.6053(64)$[M+H-Xyl]^+$, 1049.5936(100)$[M+H-Glc]^+$, 917.5442(34)$[M+H-Xyl-Glc]^+$, 785.5079(82)$[M+H-Xyl-GlcXyl]^+$, 623.4542(32)$[M+H-GlcXyl-GlcXyl]^+$
9	Ginsenoside-Rb_3	11.85	1079.6002$[M+H]^+$	1079.6011$[M+H]^+$	0.83	1043.6021(27)$[M+H-H_2O]^+$, 947.5543(32)$[M+H-Xyl]^+$, 917.5489(68)$[M+H-Glc]^+$, 785.5028(100)$[M+H-Glc-Xyl]^+$, 623.4528(35)$[M+H-Glc-GlcXyl]^+$
10	Ginsenoside-Rc	12.26	1079.6002$[M+H]^+$	1079.6027$[M+H]^+$	2.32	947.5633(38)$[M+H-Ara]^+$, 911.5621(82)$[M+H-Ara-2H_2O]^+$, 785.5124(17)$[M+H-Ara-Glc]^+$, 767.4987(100)$[M+H-Ara-Glc-H_2O]^+$, 623.4592(15)$[M+H-Ara-GlcGlc]^+$
11	Ginsenoside-Rd	12.97	947.5579$[M+H]^+$	947.5557$[M+H]^+$	2.32	929.5521(43)$[M+H-H_2O]^+$, 785.5032(100)[M+H-Glc]+, 767.5037(9)$[M+H-Glc-H_2O]^+$, 623.4514(76)$[M+H-Glc-Glc]^+$, 461.3921(57)$[M+H-GlcGlc-Glc]^+$
12	Ginsenoside-F_2	17.87	785.5051$[M+H]^+$	785.4985$[M+H]^+$	8.40	623.4450(67)$[M+H-Glc]^+$, 605.4434(100)$[M+H-Glc-H_2O]^+$, 587.4310(82)$[M+H-Glc-2H_2O]^+$, 461.7453(29)$[M+H-Glc-Glc]^+$
13	20(R)-Ginsenoside-Rg_3	18.47	785.5051$[M+H]^+$	785.4946$[M+H]^+$	13.37	623.4408(100)[M+H-Glc]+, 461.3887(39)[M+H-GlcGlc]+, 425.3821(48)$[M+H-GlcGlc-2H_2O]^+$
14	Ginsenoside-Rh_2	20.17	623.4523$[M+H]^+$	623.4507$[M+H]^+$	2.57	540.2374(84)$[M-C_6H_{11}]^+$, 461.3986(77)$[M+H-Glc]^+$, 443.3967(100)$[M+H-Glc-H_2O]^+$

15	20-*O*-glucoginsenoside-Rf	2.92	963.5529[M+H]$^+$	963.5542[M+H]$^+$	1.35	801.5035(78)[M+H−Glc]$^+$, 621.4284(100)[M+H−GlcGlc−H_2O]$^+$, 603.4288(36)[M+H−GlcGlc−2H_2O]$^+$, 477.3954(23)[M+H−GlcGlc−Glc]$^+$, 441.4041(17)[M+H−GlcGlc−Glc−2H_2O]$^{l+}$
16	Notoginsenoside-R_1	3.35	933.5423[M+H]$^+$	933.5434[M+H]$^+$	1.18	801.5051(60)[M+H−Xyl]$^+$, 771.4913(100)[M+H−Glc]$^+$, 639.4431(49)[M+H−Xyl−Glc]$^+$, 621.4483(60)[M+H−Xyl−Glc−H_2O]$^+$, 477.7496(37)[M+H−XylGlc−Glc]$^+$
17	Ginsenoside-Rg_1	3.59	801.5001[M+H]$^+$	801.4904[M+H]$^+$	12.10	639.8921(65)[M+H−Glc]$^+$, 621.8903(100)[M+H−Glc−H_2O]$^+$, 477.7514(38)[M+H−GlcGlc]$^+$
18	Ginsenoside-Re	3.62	947.5579[M+H]$^+$	947.5575[M+H]$^+$	0.42	801.4967(100)[M+H−Rha]$^+$, 785.5054(77)[M+H−Glc]$^+$, 639.4451(35)[M+H−Rha−Glc]$^+$, 603.4451(72)[M+H−Rha−Glc−2H_2O]$^+$, 477.1841(30)[M+H−Rha−GlcGlc]$^+$
19	Notoginsenoside-R_2	7.21	771.4895[M+H]$^+$	771.4862[M+H]$^+$	4.28	639.4401(54)[M+H−Xyl]$^+$, 609.4347(100)[M+H−Glc]$^+$, 477.3912(22)[M+H−Xyl−Glc]$^+$, 457.7413(8)[M+H−GlcGlc−GlcGlc−H_2O]$^+$
20	Ginsenoside-R_f	7.99	801.5000[M+H]$^+$	801.5012[M+H]$^+$	1.50	639.4473(84)[M+H−Glc]$^+$, 621.4410(100)[M+H−Glc−H_2O]$^+$, 477.3988(5)[M+H−GlcGlc]$^+$
21	Ginsenoside-Rg_2	8.42	785.5051[M+H]$^+$	785.5024[M+H]$^+$	3.44	639.4417(49)[M+H−Rha]$^+$, 621.4434(100)[M+H−Rha−H_2O]$^+$, 477.3929(51)[M+H−Rha−Glc]$^+$
22	Ginsenoside-F_1	11.20	639.4472[M+H]$^+$	639.4412[M+H]$^+$	9.38	477.3887(100)[M+H−Glc]$^+$, 441.3843(79)[M+H−Glc−2H_2O]$^+$
23	Notoginsenoside-H	3.40	949.5372[M+H]$^+$	949.5350[M+H]$^+$	2.32	817.4925(76)[M+H−Xyl]$^+$, 655.4386(100)[M+H−Xyl−Glc]$^+$, 619.4322(38)[M+H-Xyl−Glc−2H_2O]$^+$, 493.3864(55)[M+H−GlcXyl−Glc]$^+$
24	Notoginsenoside-A	6.76	1125.6057[M+H]$^+$	1125.6032[M+H]$^+$	2.22	963.5538(78)[M+H−Glc]$^+$, 801.4965(58)[M+H−GlcGlc]$^+$, 783.4942(100)[M+H−GlcGlc−H_2O]$^+$, 477.3932(25)[M+H−GlcGlc−GlcGlc]$^+$
25	Notoginsenoside-B	7.06	1123.5900[M+H]$^+$	1123.5923[M+H]$^+$	2.05	961.5591(83)[M+H−Glc]$^+$, 799.4989(41)[M+H−GlcGlc]$^+$, 763.4942(100)[M+H−GlcGlc−2H_2O]$^+$, 457.7323(18)[M+H−GlcGlc−GlcGlc−H_2O]$^+$

In parallel, all these marker ions obtained from loadings plot of PCA should be validated at a univariate level. Since each peak detected has been normalized to alleviate the effects of possible discrepancy and systematic bias ([Wang et al., 2004a] and [Webb-Robertson et al., 2005]), the PCA loadings are in good agreement with the variation of relative concentration, instead of variation of absolute content for a particular composition. A total of nine compounds with higher loadings identified were listed in the Supplementary data (Table S2) for better understanding of the separation among groups in PCA scores plot. For example, the absolute content of Rb_1**4** was slightly higher in the flower buds than in rhizomes/roots, although loading in PC1 was in good accordance with relative content of Rb_1**4**. Analogously, the relative concentration of Rd **11** was larger in rhizomes/roots than in flower buds, which is consistent with the loading in PC1.

Potential mechanism for different metabolic phenotype

During the general process of ginsenoside biosynthesis, the triterpene aglycone of ginsenoside, proopanaxadiol, is able to be synthesized from 2,3-oxidosqualene that is synthesized via the mevalonate pathway in the cytosol. Protopanaxadiol is subsequently converted to protopanaxatriol by a member of the cytochrome P450 family. Different ginsenosides are

ultimately synthesized by adding one or several monosaccharides to these triterpene aglycones via glycosyltransferase (Haralampidis et al., 2002 and Suzuki et al., 2002). Thus, activity and/or the amount of cytochrome P450 may lead to the varied contents of protopanaxadiol and protopanaxatriol type saponin among the root, rhizome and flower bud of *P. notoginseng*. Additionally, the second key enzyme during the ginsenoside biosynthesis process is saponin glycosyltransferase with the ability to catalyze the adduction of monosaccharides to sapogenins, the saponin aglycone substrate (Choi et al., 2005), suggesting that the saponins with diversity of glycosyl probably attribute to the different saponin glycosyltransferase in the different parts of *P. notogensing*. However, further investigations are necessary for clearly elucidating whether certain genes and enzymes are involved in the ultimate metabolite phenotype.

CONCLUSIONS

UPLC–ESI-MS was used for metabolite profiling of saponins in *P. notoginseng*, which is applicable for analysis and evaluation of complex herbal medicines. Furthermore, the proposed analytical method coupled with multivariate statistical analysis technique is used as a powerful tool to differentiate phytochemical compositions among different parts of *P. notoginseng*. In addition, UPLC–QtofMS performed systematic identification of tentative markers of *P. notoginseng* using accurate mass and tandem MS. The chemical compounds accountable for the different metabolite profiles of the three parts are notoginsenoside R_4**2**, Fa **3**, Q **5**, S **6**, Fc **8**, R_1**16**, H **23**, A**24**, B **25**, ginsenoside Rb_1**4**, Rb_2**7**, Rb_3**9**, Rc **10**, Rd **11**, F_2**12**, Rh_2**14**, Rg_1**17**, Re **18**, R_f**20**, Rg_2**21**, malonyl-ginsenoside-Rb_1**1** and 20-*O*-glucoginsenoside-R_f**15**, all of which are significantly up- or down- regulated in different parts of the plant. Thus, such a UPLC–ESI-MS-based metabolite profiling strategy is promising for revealing and elucidating the metabolic outcomes as a result of genetic diversity, seasonal and geographical variations, and different cultivation methods employed. Hence, this work is of great importance for the evaluation of overall quality of medicinal plants, ultimately of great significance in the pharmacological and clinical investigation of drug products of plant origin.

EXPERIMENTAL

Plant materials

A total of seven flower buds, eight roots and six rhizomes of *P. notoginseng* were collected from Wenshan Prefecture, Yunnan Province, PR China. The different parts of *P. notoginseng* were identified by Mengyue Wang, Ph.D. of Pharmacognoy, Shanghai Jiao Tong University, PR China.

Reagents and standards

Notoginsenoside R_1**16**, ginsenoside Rb_1**4**, Rg_1**17** and Re **18** standards were purchased from the National Institute for the Pharmaceutical and Biological Products (Beijing, PR China), whereas ginsenoside Rb_2**7**, Rb_3**9**, Rc **10**, Rd **11** and F_2**12** standards were obtained from Sanqi Research Institute of Wenshan Prefecture (Wenshan, Yunnan Province, PR China). Notoginsenoside R_2**18**, ginsenoside Rh_2**14**, 20(R)–Rg_3**13**, Rg_2**21**, and F_1**22** were procured from Wuhu DELTA Co. (Wuhu, Anhui Province, RP China). HPLC-grade CH_3CN was purchased from Merck Company (Darmstadt, Germany), whereas leucine-enkephalin and HCO_2H were obtained from Sigma–Aldrich (St. Louis, MO, USA). Ultra-pure H_2O was prepared with the Sartorius Arium611UF water purification system (Sartorius, Göttingen, Germany).

Sample preparation

A total of 20 mg of different parts of *P. notoginseng* were individualy added into centrifuge tube (2 ml) containing MeOH-H_2O (1 ml, 7:3, v/v), briefly shaken for 30 s, and ultrasonicated for 1 h at 50 °C for three times. The combined MeOH extracts, after removing the solvent in vacuo, were dissolved in MeOH-H_2O (1 ml, 7;3, v/v), of which 100 μl was diluted to 1 ml and filtered through a 0.22 μm filter (Millipore, MA, USA) prior to injection into the UPLC system.

Liquid chromatography

The UPLC–ESI-MS system was performed on an ACQUITY UPLC™ system (Waters Co., MA, USA), equipped with a binary solvent delivery system and an autosampler. Chromatographic separation was carried out on an ACQUITY UPLC™ BEH C_{18} column (50 mm × 2.1 mm, 1.7 μm particle size) (Waters Co., MA, USA). The column was maintained at 40 °C. The mobile phase consisted of 0.01% HCO_2H in H_2O as solvent A and CH_3CN as solvent B. Separation was performed by gradient elution: 0 min 90% A, 3 min 75% A, 10 min 70% A, 16 min 65% A, 18 min 50% A and 21 min 35% A with the flow rate of 0.35 ml/min. The injection volume of the test sample was 5 μl. Each wash cycle consisted of 200 μl of strong wash solvent (90% CH_3CN-H_2O, 9:1, v/v) and 600 μl of weak wash solvent (10% CH_3CN-H_2O, 1:9, v/v).

Mass spectrometry

Mass spectrometry was carried out on a Micromass-ZQ mass spectrometer (Waters Co., MA, USA). ESI mass spectra were acquired in positive ion electrospray ionization mode by scanning over the *m*/*z* range 400–1400. The ESI capillary voltage was set at 3.0 kV. The temperatures of electrospray source and desolvation gas were 100 °C and 300 °C, respectively. N_2 was used as the nebulizing gas, desolvation gas and cone gas at the flow-rates of 60, 600 and 50 l/h, respectively. The cone voltage varied over the range 25–90 V to investigate the intensities and distribution of ions in the mass spectra of ginsenosides.

Accurate mass measurement and MS/MS spectrometry were performed to identify ion markers using a Q-tof Premier™ mass spectrometer (Waters Co., MA, USA). Leucine-enkephalin was used as independent reference lock-mass ions via the LockSpray™ to ensure mass accuracy and reproducibility. For ES+, $[M+H]^+$ ion of leucine-enkephalin at 556.2771 Da was used as the lock mass. The concentration and the infusion flow rate of leucine-enkephalin were 50 pg/ml and 10 μl/min, respectively. The tof mass spectrometer was operated in the 'V' mode and the optimized condition was in consistent with the aforementioned ES+ mode with the exception of tof flight tube voltage 7200 V, reflectron voltage 1800 V, pusher voltage 922 V, puller voltage 750 V and MCP detector voltage 1900 V, respectively. The collision energy was set from 6 V to 10 V.

Data analysis

The UPLC–ESI-MS data of different parts of *P. notoginseng* samples were analyzed to identify potential discriminant variables. The peak finding, peak alignment, and peak filtering of ES+ raw data were carried out with MarkerLynx applications manager version 4.1 (Waters, Manchester, UK) where all the mathematical parameters are set according to our laboratory custom standards. The resulting three-dimensional matrix containing arbitrarily assigned peak index, retention time, and normalized peak area were further exported to SIMCA-P software 11.0 (Umetrics, Umeå, Sweden) for multivariate statistical analysis. PCA scores plot was employed to depict the general

clustering and groupings on the basis of the metabolic profiles, and the corresponding loadings plot was to interpret the variations among the samples.

REFERENCES

Akerele, O., 1992. WHO guidelines for the assessment of herbal medicines. Fitoterapia 63, 99–104.

Anterola, A.M., Lewis, N.G., 2002. Trends in lignin modification: a comprehensive analysis of the effects of genetic manipulations/mutations on lignification and vascular integrity. Phytochemistry 61, 221–294.

Chan, E.C.Y., Yap, S.L., Lau, A.J., Leow, P.C., Toh, D.F., Koh, H.L., 2007. Ultraperformance liquid chromatography/time-of-flight mass spectrometry based metabolomics of raw and steamed *Panax notoginseng*. Rap. Commun. Mass Spectrom. 21, 519–528.

Chang, W.T., Thissen, U., Ehlert, K.A., Koek, M.M., Jellema, R.H., Hankemeier, T., Van Der Greef, J., Wang, M., 2006. Effects of growth conditions and processing on Rehmannia glutinosa using fingerprint strategy. Planta Med. 72, 458–467.

Choi, D.W., Jung, J., Ha, Y.I., Park, H.W., In, D.S., Chung, H.J., Liu, J.R., 2005. Analysis of transcripts in methyl jasmonate-treated ginseng hairy roots to identify genes involved in the biosynthesis of ginsenosides and other secondary metabolites. Plant Cell Rep. 23, 557–566.

Cicero, A.F.G., Vitale, G., Savino, G., Arletti, R., 2003. *Panax notoginseng* (Burk.) effects on fibrinogen and lipid plasma level in rats fed on a high-fat diet. Phytother. Res. 17, 174–178.

Cloarec, O., Dumas, M.E., Trygg, J., Craig, A., Barton, R.H., Lindon, J.C., Nicholson, J.K., Holmes, E., 2005. Evaluation of the orthogonal projection on latent structure model limitations caused by chemical shift variability and improved visualization of biomarker changes in 1H NMR spectroscopic metabonomic studies. Anal. Chem. 77, 517–526.

Cui, M., Song, F., Liu, Z., Liu, S., 2001. Metal ion adducts in the structural analysis of ginsenosides by electrospray ionization with multi-stage mass spectrometry. Rap. Commun. Mass Spectrom. 15, 586–595.

Dong, L.G., He, G.Z., 2006. Application of metabonomics in clinical nutrition. Chin. J. Clin. Nutr. 14, 238–242.

Eriksson, L., Johansson, E., Kettaneh-Wold, N., Wold, S., 2001. Multi- and Megavariate Data Analysis. Umetrics Academy Umeaº, Sweden.

Farag, M.A., Huhman, D.V., Lei, Z., Sumner, L.W., 2007. Metabolic profiling and systematic identification of flavonoids and isoflavonoids in roots and cell suspension cultures of

Medicago truncatula using HPLC–UV–ESI-MS and GC–MS. Phytochemistry 68, 342–354.

Fiehn, O., 2002. Metabolomics – the link between genotypes and phenotypes. Plant Mol. Biol. 48, 155–171.

Fukusaki, E., Jumtee, K., Bamba, T., Yamaji, T., Kobayashi, A., 2006. Metabolic fingerprinting and profiling of Arabidopsis thaliana leaf and its cultured cells T87 by GC/MS. Z. Naturforschung 61, 267–272.

Guan, J., Lai, C.M., Li, S.P., 2007. A rapid method for the simultaneous determination of 11 saponins in *Panax notoginseng* using ultra-performance liquid chromatography. J. Pharm. Biomed. Anal. 44, 996–1000.

Haralampidis, K., Trojanowska, M., Osbourn, A.E., 2002. Biosynthesis of triterpenoid saponins in plants. Adv. Biochem. Eng. Biotechnol. 75, 31–49.

Huhman, D.V., Sumner, L.W., 2002. Metabolic profiling of saponins in Medicago sativa and Medicago truncatula using HPLC coupled to an electrospray ion-trap mass spectrometer. Phytochemistry 59, 347–360.

IIka, N.A., Paulo, M., Marcos, N.E., Marco António, T.Z., Alexandra, C.H.F.S., 2007. Characterization of the variation in the imidazole alkaloid profile of Pilocarpus microphyllus in different seasons and parts of the plant by electrospray ionization mass spectrometry fingerprinting and identification of novel alkaloids by tandem mass spectrometry. Rap. Commun. Mass Spectrom. 21, 1205–1213.

Konoshima, T., Takasaki, M., Tokuda, H., 1999. Anti-carcinogenic activity of the roots of *Panax notoginseng* II. Biol. Pharm. Bull. 22, 1150–1152.

Li, L., Zhang, J.L., Sheng, Y.X., Guo, D.A., Wang, Q., Guo, H.Z., 2005a. Simultaneous quantification of six major active saponins of *Panax notoginseng* by high-performance liquid chromatography–UV method. J. Pharm. Biomed. Anal. 38, 45–51.

Li, L., Tsao, R., Dou, J., Song, F., Liu, Z., Liu, S., 2005b. Detection of saponins in extract of *Panax notoginseng* by liquid chromatography–electrospray ionisation-mass spectrometry. Anal. Chim. Acta 536, 21–28.

Liu, J.H., Wang, X., Cat, S.Q., Komatsu, K., Namba, T., 2004. Analysis of the constituents in the Chinese drug notoginseng by liquid chromatography–electrospray mass spectrometry. J. Chin. Pharm. Sci. 13, 225–237.

Liu, Y., Yang, J., Cai, Z., 2006. Chemical investigation on Sijunzi decoction and its two major herbs Panax ginseng and Glycyrrhiza uralensis by LC/MS/MS. J. Pharm. Biomed. Anal. 41, 1642–1647.

Long, M., Millar, D.J., Kimura, Y., Donovan, G., Rees, J., Fraser, P.D., Bramley, P.M., Bolwell, G.P., 2006. Metabolite profiling of carotenoid and phenolic pathways in mutant and transgenic lines of tomato: identification of a high antioxidant fruit line. Phytochemistry 67, 1750–1757.

Ma, L.Y.W.C.L., Zhang, Q., Du, L.J., Chen, J.M., Xiao, P.G., 1998. Effects of PNS on blood supply and on energy metabolism in mice's brain tissues. Chin. Pharmacol. Bull. 14, 27–29.

Murch, S.J., Rupasinghe, H.P.V., Goodenowe, D., Saxena, P.K., 2004. A metabolomics analysis of medicinal diversity in Huang-qin (Scutellaria baicalensis Georgi) genotypes: discovery of novel compounds. Plant Cell Rep. 23, 419–425.

Ng, T.B., 2006. Pharmacological activity of Sanchi-Ginseng (*Panax notoginseng*). J. Pharm. Pharmacol. 58, 1007–1019.

Rochfort, S., 2005. Metabolomics reviewed: a new ''omics" platform technology for systems biology and implications for natural products research. J. Nat. Prod. 68, 1813–1820.

Sun, H., Yang, Z., Ye, Y., 2006. Structure and biological activity of protopanaxatrioltype saponins from the roots of *Panax notoginseng*. Int. Immunopharmacol. 6, 14–25.

Suzuki, H., Achnine, L., Xu, R., Matsuda, S.P.T., Dixon, R.A., 2002. A genomics approach to the early stages of triterpene saponin biosynthesis in Medicago truncatula. Plant J. 32, 1033–1048.

Taniyasu, S., Tanaka, O., Yang, T.R., Zhou, J., 1982. Dammarane saponins of flower buds of *Panax notoginseng* (Sanchi-Ginseng). Planta Med. 44, 124–125.

Wan, J.B., Yang, F.Q., Li, S.P., Wang, Y.T., Cui, X.M., 2006. Chemical characteristics for different parts of *Panax notoginseng* using pressurized liquid extraction and HPLC-ELSD. J. Pharm. Biomed. Anal. 41, 1596–1601.

Wang, X.Y., Zhang, J.T., 2003. Effect of ginsenoside Rb1 on long-term potentiation in the dentate gyrus of anaesthetized rats. J. Asian Nat. Prod. Res. 5, 1–4.

Wang, J., Ma, J.Z., Li, M.D., 2004a. Normalization of cDNA microarray data using wavelet regressions. Comb. Chem. High Throughput Screen. 7, 783–791.

Wang, Y., Tang, H., Nicholson, J.K., Hylands, P.J., Sampson, J., Whitcombe, I., Stewart, C.G., Caiger, S., Oru, I., Holmes, E., 2004b. Metabolomic strategy for the classification and quality control of phytomedicine: a case study of chamomile flower (Matricaria recutita L.). Planta Med. 70, 250–255.

Wang, M., Lamers, R.J.A.N., Korthout, H.A.A.J., Van Nesselrooij, J.H.J., Witkamp, R.F., Van Der Heijden, R., Voshol, P.J., Havekes, L.M., Verpoorte, R., Van Der Greef, J., 2005.

Metabolomics in the context of systems biology: bridging traditional chinese medicine and molecular pharmacology. Phytother. Res. 19, 173–182.

Wang, C.Z.M.E., Wicks, S., Wu, J.A., Yuan, C.S., 2006a. Phytochemical and analytical studies of *Panax notoginseng* (Burk.) F.H. Chen. J. Nat. Med. 60, 97–106.

Wang, S., Ye, S., Cheng, Y., 2006b. Separation and on-line concentration of saponins from *Panax notoginseng* by micellar electrokinetic chromatography. J. Chromatogr. A 1109, 279–284.

Webb-Robertson, B.-J.M., Lowry, D.F., Jarman, K.H., Harbo, S.J., Meng, Q.R., Fuciarelli, A.F., Pounds, J.G., Lee, K.M., 2005. A Study of spectral integration and normalization in NMR-based metabonomic analyses. J. Pharm. Biomed. Anal. 39, 830–836.

Wei, J.X., Du, Y.C., 1996. Modern Science Research and Application of Panax notoginseng. Yunnan Science and Technology Press, Kunming, China.

Wilson, I.D., Nicholson, J.K., Castro-Perez, J., Granger, J.H., Johnson, K.A., Smith, B.W., Plumb, R.S., 2005. High resolution ultra-performance liquid chromatography coupled to oa-TOF mass spectrometry as a tool for differential metabolic pathway profiling in functional genomic studies. J. Proteome Res. 4, 591–598.

Xiao, P., 2002. Modern Chinese Materia Medica. Chemical Industry Press, Beijing.

Xu, Y.X., Shi, J.S., Jiang, Z.L., 2005. Inhibitory influence of ginsenoside Rb3 on activation of strychnine-sensitive glycine receptors in hippocampal neurons of rat. Brain Res. 1037, 99–106.

Yoshikawa, M., Morikawa, T., Kashima, Y., Ninomiya, K., Matsuda, H., 2003. Structures of new dammarane-type triterpene saponins from the flower buds of *Panax notoginseng* and hepatoprotective effects of principal ginseng saponins. J. Nat. Prod. 66, 922–927.